Materials Science and Engineering A 527 (2010) 752–760

Contents lists available at ScienceDirect

Materials Science and Engineering A

journal homepage: www.elsevier.com/locate/msea

Principles of self-annealing in silver processed by equal-channel angular pressing: The significance of a very low stacking fault energy

Jenő Gubicza[a,*], Nguyen Q. Chinh[a,b], János L. Lábár[a,c], Zoltán Hegedűs[a], Terence G. Langdon[b,d]

[a] Department of Materials Physics, Eötvös Loránd University, Pázmány Péter s. 1/A, H-1117 Budapest, Hungary
[b] Department of Aerospace & Mechanical Engineering and Materials Science, University of Southern California, Los Angeles, CA 90089-1453, USA
[c] Research Institute for Technical Physics and Materials Science, P.O. Box 49, H-1525 Budapest, Hungary
[d] Materials Research Group, School of Engineering Sciences, University of Southampton, Southampton SO17 1BJ, UK

ARTICLE INFO

Article history:
Received 15 June 2009
Received in revised form 22 August 2009
Accepted 26 August 2009

Keywords:
Severe plastic deformation
Equal-channel angular pressing
Ultrafine-grained materials
Recovery
Recrystallization
Stacking fault energy

ABSTRACT

Experiments were conducted to evaluate the long-term microstructural stability of silver after processing using equal-channel angular pressing (ECAP). The results show that an ultrafine-grained microstructure is produced by ECAP at room temperature but there is self-annealing in the form of recovery and recrystallization during long-term storage at room temperature. In practice, the very low stacking fault energy of silver results in a high degree of dislocation dissociation and thereby hinders recovery by cross-slip and climb. The experiments examine the evolution of microstructure and the mechanical behavior as a function of the storage time after different numbers of ECAP passes. The results demonstrate that the degree and kinetics of self-annealing depend upon the number of passes imposed in ECAP.

1. Introduction

Bulk nanocrystalline (NC) and ultrafine-grained (UFG) materials are currently a major focus in materials science due to their unique properties in comparison to their coarse-grained counterparts [1–3]. Specifically, an important feature of NC and UFG materials is their high strength at ambient temperatures. In practice, the long-term stability of these UFG microstructures is an important prerequisite if these materials are used in any industrial applications. Thus, if the fine grains become coarsened during their service lifetime, their unique properties including their high strength will be lost.

It is generally considered that NC and UFG materials are reasonably stable at their production temperature. Nevertheless, it was shown for nanocrystalline Cu and Ag layers, having a thickness of ~1–20 μm and processed by electroplating, that recrystallization occurs at room temperature (RT) within ~1–2 days of their production [4–7]. This phenomenon is known as "self-annealing". It was suggested that during layer processing the organic additives reduce the interfacial energy anisotropically and additionally pin the grain boundaries thereby stabilizing the small grain size [4,5]. However, the additives disappear from the layers in several hours after plating and this increases the grain boundary energy and leads to an increased driving force for recrystallization. Nanocrystalline Cu and Ag samples processed by the consolidation of nanopowders also show self-annealing at RT during periods of several days after their production [8,9].

One of the most frequently used method for producing bulk UFG metals by severe plastic deformation (SPD) is equal-channel angular pressing (ECAP) where it is possible to produce materials having dimensions of several centimeters in all directions [10]. These materials also exhibit self-annealing and it was shown recently that the UFG microstructure in Cu samples processed by ECAP at RT becomes partially recrystallized during storage at the temperature of processing [11–13]. For example, large recrystallized grains were observed in 99.96% purity Cu 8 years after processing by ECAP [13]. Experiments on 5N purity Cu showed that recrystallization occurred only 2 months after ECAP and the lower recrystallization time for the pure material was explained by the non-availability of the pinning effect of alloying elements on grain boundaries and dislocations [11]. There is also a similar report of partial recrystallization in the severely deformed surface region of a thin wire-drawn copper, having a diameter of 0.1 mm, where this was strongly affected by the impurity concentration [14].

An earlier study reported experiments on pure Ag where the stacking fault energy (SFE) is very low (~16 mJ m^{-2} [15]) and the

* Corresponding author. Tel.: +36 1 372 2876; fax: +36 1 372 2811.
E-mail address: gubicza@metal.elte.hu (J. Gubicza).

0921-5093/$ – see front matter © 2009 Elsevier B.V. All rights reserved.
doi:10.1016/j.msea.2009.08.071

dislocation density after 8 ECAP passes was $\sim 46 \pm 5 \times 10^{14}\,m^{-2}$ which is very high by comparison with other fcc metals such as Al, Au or Cu [16]. This exceptionally high dislocation density is a direct consequence of the very low SFE of Ag because the annihilation of dislocations is hindered by their high degree of dissociation into partials. The result also matches reports on the alloying of Cu with Zn where there is a large increase in the dislocation density due to the reduction of SFE with increasing Zn concentration [17,18]. Some earlier experiments on Ag showed self-annealing of the UFG microstructure at RT which occurred several months after processing through 8 passes of ECAP [19].

The present investigation was initiated to provide a detailed evaluation of the significance of self-annealing in Ag of 99.99% purity when processing by ECAP. The evolution of the microstructure and the consequent mechanical properties were systematically investigated as a function of the time of storage following processing by ECAP through totals from 1 to 16 passes.

2. Experimental material and procedures

High-purity 99.99% Ag billets having lengths of ~70 mm and diameters of ~10 mm were homogenized for 60 min at a temperature of 741 K (corresponding to $0.6T_m$, where T_m is the absolute melting point of Ag). Following homogenization, these billets were pressed through totals of 1, 4, 8 and 16 passes of ECAP using route B_C at room temperature with a pressing velocity of 8 mm s^{-1} and a solid die having an internal channel angle of 90° and an outer arc of curvature of ~20° at the intersection of the two parts of the channel. In this configuration, one pass corresponds to an equivalent strain of ~1 [20]. Following ECAP, the billets were stored at RT and the microstructures and mechanical behavior were examined as a function of the time of storage for periods up to a total of 4 months.

Microstructures were examined periodically by X-ray line profile analysis on transverse sections cut perpendicular to the axes of the billets. The measurements of the X-ray diffraction lines were performed using a special high-resolution diffractometer (Nonius FR591) with CuKα_1 radiation ($\lambda = 0.15406$ nm). The line profiles were evaluated using the extended Convolutional Multiple Whole Profile (eCMWP) fitting procedure [21]. In this method, the diffraction pattern is fitted by the sum of a background spline and theoretical peak profiles. The profile functions are calculated as the convolution of the theoretical size and strain peak profiles. In addition, the theoretical size and strain peak profile functions are calculated on the basis of a model of the microstructure. Based on this model, the crystallites have spherical shape and log-normal size distribution, and the lattice strains are assumed to be caused by dislocations and twins. This method gives both the dislocation density and the twin fault probability with good statistics, where the twin fault probability is defined as the fraction of the faulted {1 1 1} planes along their normal vector. The microstructures of selected samples were examined using a Philips CM-20 transmission electron microscope (TEM) operating at 200 kV. The TEM samples were mechanically thinned to ~80 μm, cooled to liquid nitrogen temperature and then thinned with 6 keV Ar^+ ions from both sides until perforation. Finally, a thin damaged layer was removed using 2 keV Ar^+ ions.

The hardness of the samples was measured using a Vickers microhardness indenter in a Shimadzu-DUH 202 machine with an applied load of 2000 mN. The deformation behavior was studied using uniaxial compression testing with a computer-controlled hydraulic mechanical testing MTS 810 machine. For all of these tests, the direction of compression was parallel to the longitudinal axis of each billet.

3. Experimental results

3.1. Characterization of the microstructure in silver immediately after ECAP

The initial mean grain size of the Ag samples was ~10 μm prior to ECAP but this was reduced to ~5 μm after 1 pass of ECAP. The TEM image in Fig. 1(a) demonstrates that the grains contain both dislocations and twins after processing through 1 pass, where some of the twin boundaries are denoted by white arrows. The dislocation density and the probability of twins were estimated after 1 pass as $\sim 16 \pm 2 \times 10^{14}\,m^{-2}$ and $\sim 0.1 \pm 0.1\%$, respectively, as determined from X-ray line profile analysis. After 4 passes, the grain size decreased to $\sim 160 \pm 50$ nm as shown in Fig. 1(b) and the grain size remained essentially unchanged within experimental error after 8 passes (200 ± 50 nm) and 16 passes (190 ± 50 nm) as illustrated in Fig. 1(c) and (d), respectively. This invariance with increasing numbers of ECAP passes matches recent detailed measurements taken on a high-purity (99.99%) aluminum processed by ECAP through 4–12 passes [22].

Measurements using X-ray line profile analysis after 4 passes showed increases in the dislocation density and the twin probability to $\sim 37 \pm 4 \times 10^{14}\,m^{-2}$ and $\sim 0.7 \pm 0.1\%$, respectively. The dislocation density saturated after 8 passes at $\sim 46 \pm 5 \times 10^{14}\,m^{-2}$ and the twin probability increased to $\sim 0.9 \pm 0.1\%$, whereas after 16 passes the dislocation density was reduced to $\sim 25 \pm 10 \times 10^{14} m^{-2}$ while the twin probability further increased to $\sim 1.5 \pm 0.1\%$. The hardness of the initial sample prior to ECAP was $\sim 0.40 \pm 0.03$ GPa but the hardness increased to $\sim 0.89 \pm 0.05$ GPa after 1 pass and a maximum hardness of $\sim 1.07 \pm 0.05$ GPa was attained after 4 passes. Thereafter, at higher numbers of passes, the measured hardness remained unchanged within experimental error.

3.2. Self-annealing of the severely deformed microstructure during storage at room temperature

Fig. 2 shows the microhardness of samples processed by different numbers of ECAP passes as a function of the time of storage at room temperature, where the lower horizontal line denotes the hardness of the initial sample. It is apparent that the hardness after 1 pass remains unchanged within experimental error even after storage for 4 months. By contrast, the hardness gradually decreases with increasing storage time for the samples processed by 4, 8 and 16 passes thereby demonstrating that the severely deformed microstructure is inherently unstable and subject to self-annealing, most probably by recovery and recrystallization, during long-term storage at room temperature.

True stress–logarithmic strain compression curves are shown in Fig. 3 for samples processed through 1, 4, 8 and 16 passes both immediately after ECAP and after 4 months in storage: for comparison, a stress–strain curve for the initial unpressed condition is also shown. Immediately after 1 pass of ECAP the stress–strain curve shows only a negligible hardening with increasing strain and the compression behavior is similar also for the samples pressed through 4, 8 and 16 passes. After storage for 4 months at RT, there is a similar stress–strain curve with negligible hardening after 1 pass of ECAP whereas the samples pressed through 4–16 passes show a reduction in the yield strength and a very significant strain hardening. This softening of the samples confirms that the change in microhardness evident in Fig. 2 is not related only to a surface effect but rather it reflects a genuine microstructural change occurring during storage at RT. The results in Fig. 3 show that the magnitude of the decrease in flow stress increases with increasing numbers of ECAP passes and this is consistent with the variation of the microhardness values recorded in Fig. 2.

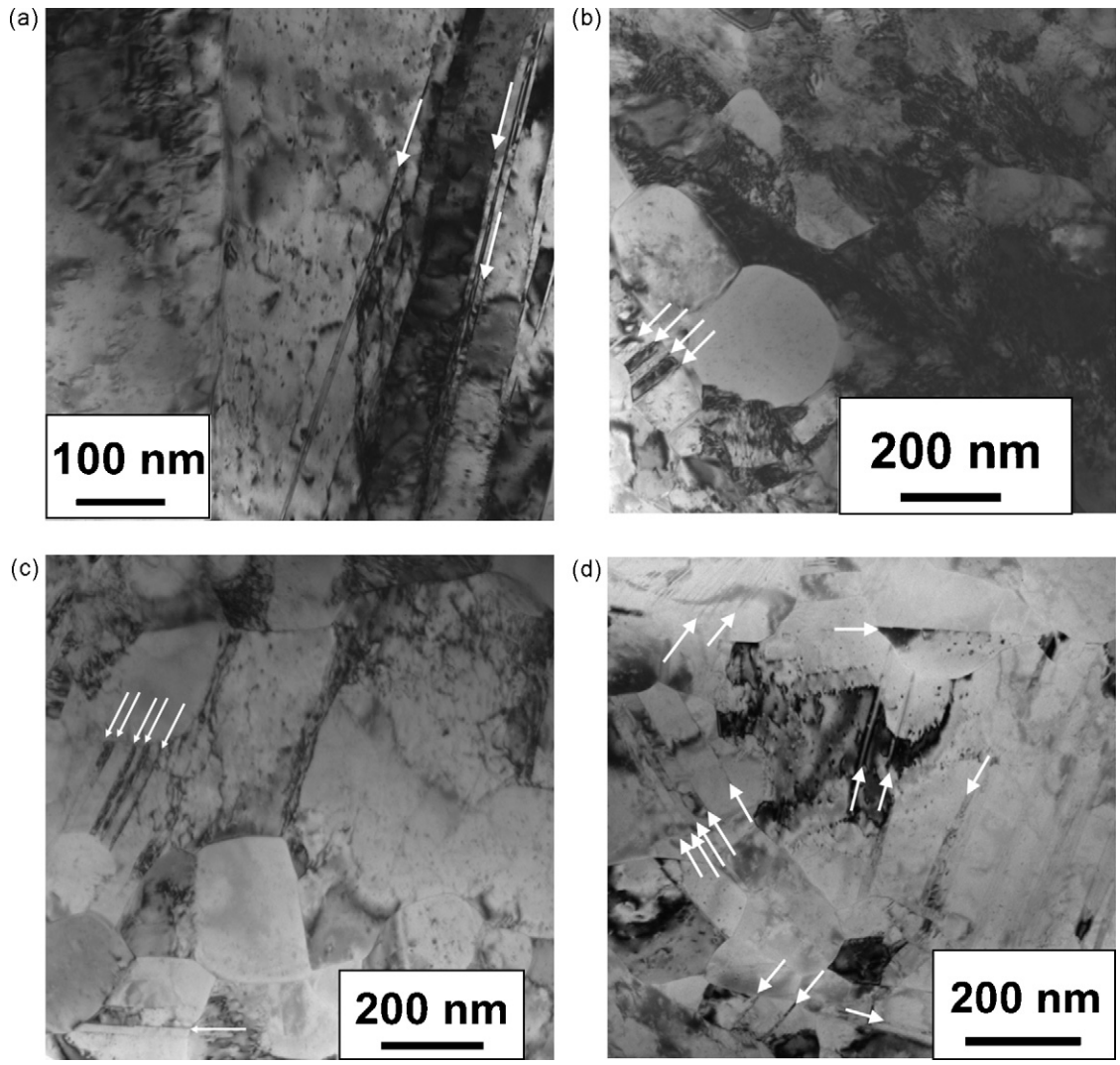

Fig. 1. TEM images taken after (a) 1, (b) 4, (c) 8 and (d) 16 passes of ECAP: examples of twin boundaries are indicated by white arrows.

The dislocation density and twin probability were determined as a function of storage time using X-ray diffraction line profile analysis. Fig. 4(a) shows a Debye–Scherrer diffraction ring of the 2 2 0 reflection obtained immediately after 8 passes of ECAP. In this condition the intensity distribution around the ring is relatively homogeneous, thereby indicating a high degree of homogeneity within the microstructure. Similar diffraction rings were also

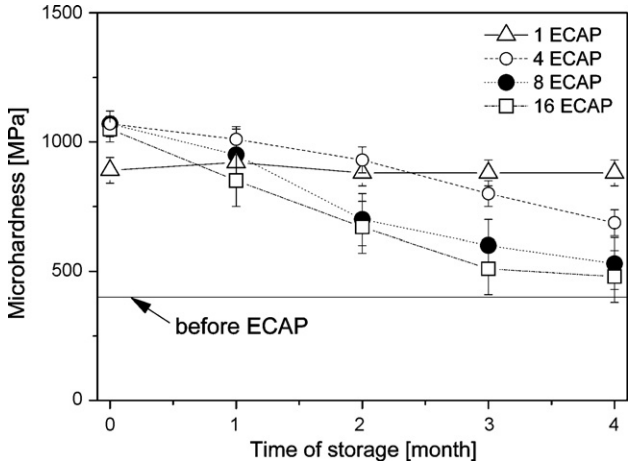

Fig. 2. Values of the microhardness after processing by ECAP for 1, 4, 8 and 16 passes as a function of the storage time at room temperature.

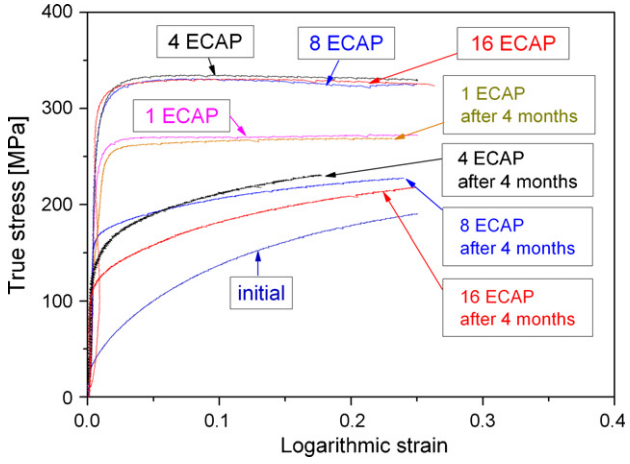

Fig. 3. True stress–logarithmic strain curves obtained on samples immediately after ECAP, and after ECAP and storage at room temperature for 4 months: a curve for the initial unpressed condition is also shown.

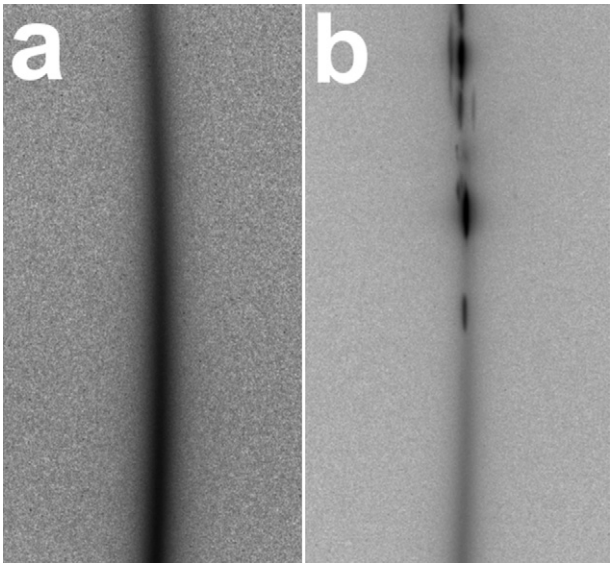

Fig. 4. Debye–Scherrer rings for the 2 2 0 reflection of X-rays (a) immediately after 8 ECAP passes and (b) after 8 ECAP passes and storage at room temperature for 4 months.

recorded for the other samples immediately after processing by ECAP. Nevertheless, there were very significant changes after 1 month of storage at RT and high intensity spots were observed on the Debye–Scherrer rings for the samples processed through 4, 8 and 16 passes. Furthermore, these irregularities in intensity became even more visible after storage for 4 months. Fig. 4(b) shows an example for the 2 2 0 reflection obtained after processing through 8 passes and storing for 4 months. The inhomogeneous intensity distributions in the Debye–Scherrer rings suggest there is a fluctuation in the degree of self-annealing within the microstructure. Since the breadths of the individual high intensity spots were close to the instrumental broadening, it was not feasible to evaluate these parts of the diffraction rings quantitatively. However, these high intensity spots are most probably scattered from recrystallized grains having larger sizes and lower dislocation densities than the detection limits of the line profile analysis (~800 nm and $\sim 10^{13}$ m^{-2} for the crystallite size and the dislocation density, respectively) and the rather homogeneous portions of the Debye–Scherrer rings are most probably related to the recovered volumes. The Debye–Scherrer rings for the samples processed for 4 and 16 passes also became inhomogeneous during storage at RT whereas the diffraction rings remained homogeneous in the sample processed by 1 pass even after storage for 4 months.

The dislocation density and the twin probability evaluated from the homogeneous portions of the rings are shown as a function of the storage time in Fig. 5(a) and (b), respectively. In this evaluation, first a large area free from large intensity spots was cut from the Debye–Scherrer ring for each reflection, then the intensity was integrated along these homogeneous parts of the rings and the received peak profiles were fitted by the CMWP procedure. For the sample processed by 1 pass the dislocation density in Fig. 5(a) remains essentially unchanged whereas after 4, 8 and 16 passes the dislocation density decreases with the time of storage but with the decrease occurring at different rates. The reduction in the dislocation density is fastest after 8 passes but stops after about 1 month when it reaches the value characteristic of the sample pressed through only 1 pass ($\sim 16 \times 10^{14}$ m^{-2}). For the specimen deformed by 4 passes, the dislocation density decreases more slowly but after 2 months it also converges to the same value. For 16 passes, the dislocation density decreases only slightly from $\sim 25 \pm 3 \times 10^{14}$ m^{-2} to $\sim 20 \pm 3 \times 10^{14}$ m^{-2} during 4 months of storage but a further

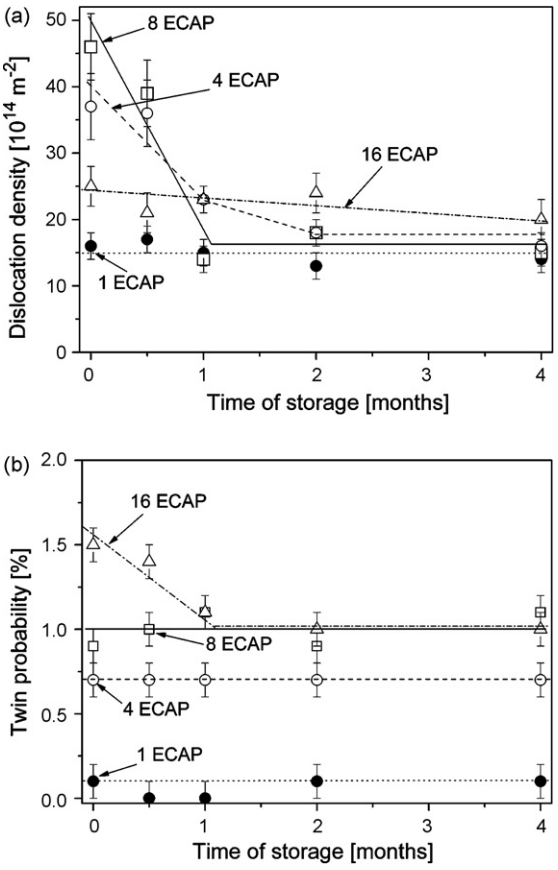

Fig. 5. (a) The dislocation density and (b) the twin probability in the recovered volumes of samples stored at room temperature for up to 4 months after processing by ECAP through 1, 4, 8 and 16 passes.

reduction during storage for a longer time cannot be excluded. It is concluded that there is a more rapid reduction during storage when there is a higher initial dislocation density. Fig. 5(b) shows that the twin probability remains practically unchanged for specimens processed through 1, 4, and 8 passes but for the 16 passes sample the twin probability decreases from $\sim 1.5 \pm 0.1\%$ to $\sim 1.1 \pm 0.1\%$ during the first month of storage and thereafter remains unchanged. It is emphasized that the defect densities plotted in Fig. 5 were determined from the homogeneous parts of the Debye–Scherrer rings which are free from the large intensity spots. Consequently, these values are characteristic only of the recovered parts of the samples and most probably the mean dislocation density and twin probability will be lower for the whole specimens because of contributions from the recrystallized fractions of the samples.

Fig. 6(a) and (b) shows bright and dark field TEM images, respectively, taken from the same area of the sample processed by 8 passes and stored for 1 month at RT: on the right sides of the images there is a large recrystallized grain with a size of ~1 μm while in the other parts of the images the grain size remains at ~200–300 nm. Fig. 6(c) shows the microstructure of the specimen processed by 8 passes and then stored for 4 months where the grains are now fully recrystallized with an average size of ~1 μm.

4. Discussion

4.1. Evolution of microstructure during processing by ECAP

The evolution of the dislocation and twin densities with increasing strain in ECAP appears to be generally consistent with the

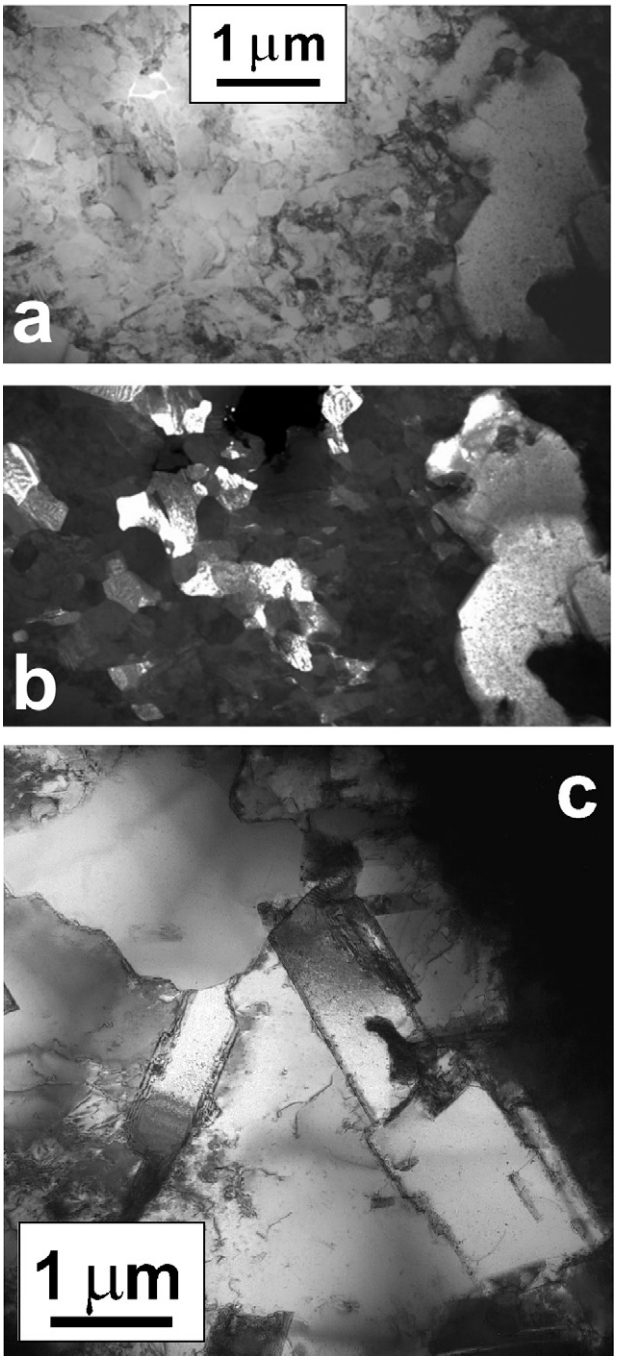

Fig. 6. (a) Bright and (b) dark field TEM images from a sample processed through 8 ECAP passes and stored at room temperature for 1 month and (c) a bright field TEM image of the same sample after storage for 4 months.

theoretical predictions of a model developed by Müllner and Solenthaler [23] for plastic straining of fcc metals and alloys having low SFE. Specifically, the deformation behavior in these materials at relatively low strains is controlled mainly by the planar glide of dissociated dislocations and the dislocation density then increases rapidly while twinning is marginal. As the deformation proceeds, dislocation pile-ups form at glide obstacles such as Lomer–Cottrell locks and grain boundaries. In fcc metals having low SFE, these glide obstacles strongly hinder the further activity of lattice dislocations because motion by climb or cross-slip is difficult due to the high degree of dislocation dissociation. Accordingly, if the local stresses at these obstacles exceed the critical stress required for twin nucleation, plasticity will continue by twinning. With increasing strain as in ECAP, the dislocation density further increases together with the locations of these high stress concentrations and this leads to an increased density of twinning. However, these twins also obstruct the glide of lattice dislocations thereby hindering the subsequent operation of dislocation sources and leading to an overall reduction in the rate of dislocation production.

In the present experiments, the dislocation density saturates at a strain of $\varepsilon \approx 8$ and for higher strains the dislocation density decreases while the twin probability continues to increase. This reduction in dislocation density at high strains is due to the nature of the twinning mechanism. Several possible mechanisms have been proposed for twin formation including by (i) a pole mechanism [24], (ii) the dissociation of lattice dislocations into Shockley and Frank partials at Lomer–Cottrell barriers [25], (iii) the nucleation of three-layer twins by dissociation of co-planar lattice dislocations into Shockley partials [26] and/or (iv) the emission of twinning partials from grain boundaries [27,28]. All of these mechanisms of twinning are based inherently on the dissociation of lattice dislocations into twinning partials such that, if the partials then move to the grain boundaries, the formation of twins will contribute to the annihilation of lattice dislocations. This means that, as a consequence, the decrease in dislocation density between 8 and 16 passes is associated with an increase in the twin concentration. It is important to note that the dislocation sources are incapable of compensating for the dislocations lost by twinning because the operation of these sources is also obstructed by the newly nucleated twins. A dynamic recovery mechanism may also contribute to the decrease in the dislocation density in Ag between 8 and 16 passes in a manner similar to that reported for Cu processed by more than 8 passes in ECAP [29]. This recovery may be performed by climb of dislocations when the internal stresses and/or concentration of deformation-induced vacancies reach critical values at high strains of SPD-processing.

It should be noted that, despite the increase of the dislocation density and twin probability between 4 and 8 passes, the hardness and the flow stress remain unchanged. This dichotomy may be explained by noting that according to X-ray line profile analysis the relative fraction of screw dislocations in the dislocation population increases with increasing strain because their annihilation is more effectively hindered by their higher degree of dissociation by comparison with edge dislocations. Thus, these screw dislocations pass through the dislocation forest more easily due to their smaller self-energy compared to edge dislocations and this leads to a similar hardness after 8 passes in spite of the higher dislocation density compared to the sample processed by 4 passes. After 16 passes, the smaller strengthening effect due to the decreased density of dislocations is effectively compensated by the higher twin probability.

4.2. The possibility of delayed recovery of the dislocation structure by cross-slip

The present experiments provide clear evidence for the self-annealing of Ag samples at RT after processing by at least 4 passes of ECAP. The X-ray diffraction and TEM results demonstrate that both delayed recovery and recrystallization occur during self-annealing. During recovery, the screw and edge dislocations are annihilated by cross-slip and climb, respectively. The probability of the occurrence of these mechanisms is dependent upon the degree of dislocation dissociation. In fcc metals the lattice dislocations are dissociated into Shockley partials bordering a ribbon of stacking fault where the equilibrium splitting distance, d, between the partials is expressed

as [30]:

$$d = A\frac{Gb^2}{\gamma}, \quad (1)$$

where G is the shear modulus, b is the Burgers vector, γ is the stacking fault energy and A is a constant having values of ~0.019 and ~0.048 for screw and edge dislocations, respectively. The values of the equilibrium splitting distances for screw dislocations, when expressed in terms of the Burgers vector unit d/b, were calculated using Eq. (1) from the values of G, b and γ given in Table 1 of Ref. [16]. The calculated d/b values are ~0.9, ~3.1, ~3.7, ~3.9 and ~8.7 for Al, Ni, Cu, Au and Ag, respectively. These calculations show that the splitting distance is exceptionally high in Ag because of the very low SFE.

This high degree of dislocation dissociation impedes motion by cross-slip. In the cross-slip model developed by Friedel [31], cross-slip occurs in fcc crystals by the formation of an initial constriction in the dissociated dislocation and the subsequent extension of this constricted segment onto the cross-slip plane. The cross-slip process is stress-assisted because the activation energy of the process is reduced by the shear stress, σ', pushing the partials towards each other on the initial glide plane and by the shear stress, σ_s, pulling the partials in opposite directions on the cross-slip plane. The energy, W, required for cross-slip is given by the relationship [32]:

$$W = W_0\left(1 - 1.2\frac{\sigma_s b}{\gamma} - 1.5\frac{\sigma' b}{\gamma}\right), \quad (2)$$

where W_0 is the constriction energy which is given by

$$W_0 = \frac{Gb^2 d}{37}\left(\ln\left(\frac{2\sqrt{3}d}{b}\right)\right)^{1/2}. \quad (3)$$

Although there are other slightly different relationships for the constriction energy [33,34], the order of magnitude of W_0 remains similar and all relationships predict an increasing constriction energy with increasing d/b.

The energy required for cross-slip is supplied by the thermal fluctuations occurring in the crystalline lattice. From the thermal activation of cross-slip, it follows that the waiting time for this process, t_{cs}, may be expressed as:

$$t_{cs} = \frac{1}{\nu_0}\exp\left(\frac{W}{kT}\right), \quad (4)$$

where ν_0 is the frequency for the crystal vibrations (~10^{13} Hz), k is Boltzmann's constant and T is the absolute temperature (300 K in this case). Thus, higher values of W correspond to longer waiting times for cross-slip.

The waiting times for cross-slip were calculated from Eqs. (2)–(4) for five different pure fcc metals (Al, Ni, Cu, Au and Ag). Since the values of the stresses σ' and σ_s are not known, a first approximation was adopted whereby the cross-slip energy was taken as the constriction energy, W_0. The resulting calculated values of t_{cs} are represented by the circles in Fig. 7 where the waiting time is plotted as a function of the normalized equilibrium splitting distance, d/b, for dissociated screw dislocations of these five different metals and the dotted horizontal line denotes the estimated time associated with pressing through 16 passes of ECAP (equivalent to ~10^3 s). Thus, the smallest and largest values of t_{cs} are related to the lowest and the highest degrees of dissociation in Al and Ag, respectively, and for metals having intermediate values of d/b (Ni, Cu and Au) the estimated values of t_{cs} lie between the extreme values for Al and Ag.

Fig. 7 shows that for Al, Ni, Cu and Au the waiting times for cross-slip are significantly smaller than or close to the total time for processing by ECAP through 16 passes so that the annihilation of the screw dislocations by cross-slip takes place during the ECAP processing operation. By contrast, the waiting time for cross-slip in Ag is of the order of ~10^{21} s, equivalent to a waiting period of ~10^{13} years, which means in practice that the dislocations formed during ECAP are not annihilated by cross-slip without the benefit of some assisting stresses. However, there is evidence for internal stresses in the microstructures produced by SPD due to the presence of other dislocations and in practice these internal stresses may either assist or hinder the cross-slip process.

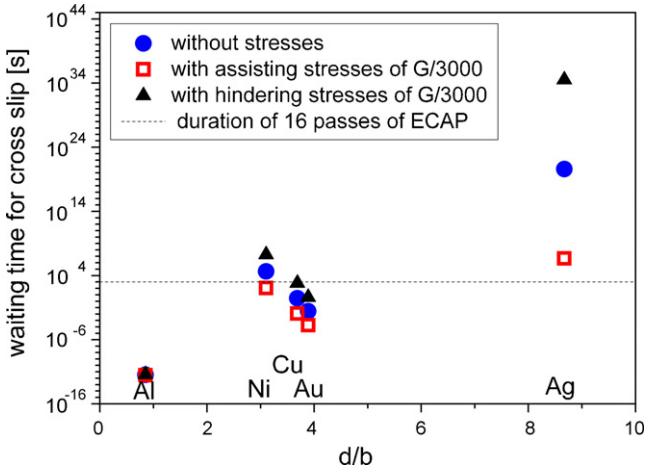

Fig. 7. The waiting time needed for cross-slip of a screw dislocation as a function of the equilibrium splitting distance between partials normalized by the Burgers vector, d/b, for the situation where cross-slip is either not assisted by stresses or where it is facilitated or hindered by shear stresses having a value of $G/3000$: the horizontal line denotes the approximate time entailed in processing through 16 passes of ECAP using a pressing velocity of 8 mm s^{-1}.

The activation energy for cross-slip is sensitive to the presence of these internal stresses. Unfortunately, no internal stress data are available in the literature for severely deformed Ag. At the same time, the residual internal stresses in deformed Cu were measured as ~$G/3000$ [35]. Taking this value for the assisting stresses, σ' and σ_s, the waiting time for cross-slip is significantly reduced for all materials as illustrated by the squares in Fig. 7. This decrease in waiting time is most significant for Ag where t_{cs} is reduced to ~10^7 s (equivalent to ~4 months). This means, therefore, that it is difficult for cross-slip to occur during ECAP of Ag so that a very high dislocation density is introduced but at the same time these dislocations may be annihilated several months after processing thereby giving a delayed recovery for the dislocation structure. The present calculation is therefore in agreement with, and provides an explanation for, the experimental data.

In severely deformed polycrystals, the magnitude and direction of the remaining stresses acting on the glide planes after deformation change from grain to grain due to the distributions of the dislocations and other defects, such as twins, so that the probability of cross-slip depends upon their specific locations within the specimen. In some locations in the microstructure the stresses may hinder cross-slip resulting in an increase in the waiting time as illustrated by the triangles in Fig. 7 for a stress value of $G/3000$. As a result of the stress distributions which are an inherent feature of all deformed materials, it is anticipated there will be fluctuations in the waiting times for dislocation annihilation.

It is apparent from Fig. 5 that higher dislocation densities after ECAP are associated with faster rates of recovery so that shorter times are then needed to achieve the stable dislocation density during storage at RT. For all ECAP samples, the stable dislocation density is close to the value obtained immediately after 1 pass (~16×10^{14} m^{-2}). For the sample processed by 16 passes, the initial dislocation density is much smaller than for 8 passes so that the recovery occurs more slowly. Furthermore, the higher

initial dislocation density corresponds to a shorter mean spacing between dislocations and therefore higher assisting stresses and consequently faster cross-slip. For the sample processed by 1 pass, the assisting stresses are sufficiently low that the microstructure remains reasonably stable within the storage time of 4 months. Considering the factor of 3 between the dislocation densities of the samples processed by 1 and 8 passes, it is estimated that the microstructure of the 1 pass sample has a higher mean spacing between dislocations by a factor of $\sqrt{3}$. As a result, the internal stresses due to dislocations in the sample after 1 pass are lower by a factor of $\sqrt{3}$ than in the sample after 8 passes. Using Eq. (4), it was calculated that this reduction of assisting stresses leads to an increase in the waiting time for cross-slip by several orders of magnitude, thereby explaining the lack of any significant recovery in the 1 pass sample and also the termination in recovery in the samples processed by 4 and 8 passes when the dislocation density reaches the value characteristic for 1 pass. It should be noted that an apparent decrease of the dislocation density in the recovered but non-recrystallized fraction of the samples may also occur if the recrystallization starts in those volumes having the highest dislocation density.

4.3. Annihilation of dissociated dislocations by climb

In addition to the cross-slip of screw dislocations, recovery may occur through the climb of edge dislocations. The climb velocity of an extended dislocation is [36]:

$$v_c = \frac{1050\sigma\Omega D}{bkT} c_j \left(\frac{d}{b}\right)^{-2}, \quad (5)$$

where σ is the stress acting across the extra half plane of the dislocation producing a climb force σb, Ω is the atomic volume, D is the diffusion coefficient and c_j is the number of jogs along the dislocation line. The characteristic waiting time for the annihilation of edge dislocations by climb, t_{climb}, may be approximated as the ratio of the mean spacing between dislocations ($\rho^{-1/2}$ where ρ is the average dislocation density) and the climb velocity so that

$$t_{climb} = \frac{\rho^{-1/2}}{v_c}. \quad (6)$$

It can be established from Eq. (5) that the velocity of climb decreases with an increase in the splitting distance between partials, d/b, and therefore dislocation dissociation also hinders annihilation by climb. Eqs. (5) and (6) show that the waiting time for climb depends quadratically on d/b but for cross-slip the waiting time depends exponentially on the splitting distance which means that cross-slip is more sensitive to an increase in the splitting distance. There is a similar effect for the stress sensitivity of the two mechanisms. For fcc metals having relatively small splitting distances (e.g. Al, Ni, Cu or Au), cross-slip is usually considered to be much faster than climb at RT [30] so that the minimum distance between dislocations, and therefore the maximum dislocation density achieved by ECAP, is determined primarily by the rate of climb. Furthermore, since climb is a diffusion-controlled mechanism, it becomes significant only at elevated temperatures where the rates of diffusion are reasonably fast. Nevertheless, experimental evidence suggests that, due to the high volume fraction of grain boundaries and large concentration of dislocations in materials processed by SPD, diffusion may be faster than in coarse-grained specimens by up to several orders of magnitude [37]. This faster diffusion suggests the possibility of a significant role for climb in the annihilation of dislocations even at RT. The velocity of climb is also enhanced by the high concentration of deformation-induced vacancies in SPD-processed materials. Since the diffusion activation energy is proportional to the absolute melting temperature, T_m, in pure fcc metals, the appropriate velocity of climb will depend strongly on T_m and this explains the observed correlation in pure fcc materials between the maximum dislocation density achieved by ECAP at room temperature and the melting temperature [38].

The characteristic waiting time for climb in Ag may be estimated by substituting appropriate values into Eqs. (5) and (6): $\sigma = G/3000$ which is similar to the value used for cross-slip, $\Omega/b = 10^{-19}\,m^2$, $c_j = 1$, $kT = 4 \times 10^{-21}\,J$, $d/b = 22$ from Eq. (1) for edge dislocations and taking $\rho = 46 \times 10^{14}\,m^{-2}$ as the value after 8 passes so that $\rho^{-1/2} = 15\,nm$. The value of the diffusion coefficient depends on the migration path of vacancies since D is $\sim 10^{-35}\,m^2\,s^{-1}$ [39] in bulk Ag and $\sim 10^{-20}\,m^2\,s^{-1}$ along grain boundaries and dislocations [40]. Due to the high dislocation density and small grain size, it is assumed that vacancy diffusion occurs predominantly along dislocations and grain boundaries so that $D \approx 10^{-20}\,m^2\,s^{-1}$ and, from Eqs. (5) and (6), $t_{climb} \approx 10^3\,s$. This value is smaller than the waiting time of $\sim 10^7\,s$ for cross-slip in Ag so that the very slow cross-slip yields a higher saturation dislocation density ($\sim 46 \times 10^{14}\,m^{-2}$) than the corresponding values for other fcc metals with similar melting points (e.g. $\sim 17 \times 10^{14}\,m^{-2}$ in Au [16]). This high dislocation density therefore leads to a large driving force for self-annealing during storage at RT.

4.4. The occurrence of recrystallization during self-annealing

The X-ray line profile analysis shows that in the recovered volumes of samples processed through 4–16 passes the dislocation density and the twin probability do not decrease below the value characteristic of the sample pressed through 1 pass (Fig. 5) while the hardness (Fig. 2) and the flow stress (Fig. 3) for the samples for 4–16 passes fall below the values for 1 pass after storage for a period of 4 months. This apparent dichotomy is readily explained by the advent of partial recrystallization in the samples processed through 4–16 passes. Indeed, the large intensity spots in the Debye–Scherrer rings (Fig. 4) and the TEM image in Fig. 6(c) indicate that, in addition to recovery of the dislocation structure, recrystallization also operates during storage at RT at least after processing through 4 passes. Since the activation energy for recovery is smaller than for recrystallization, it is anticipated that recovery will precede recrystallization. As a consequence, and as noted in other reports [41], recovery may diminish the driving force for recrystallization by reducing the dislocation density and/or by decreasing the internal stresses through dislocation rearrangement. In the samples processed by ECAP, recrystallization most probably starts at locations where there is no recovery due to the hindering stresses or where recovery is slow due to low assisting stresses and therefore the driving force remains high during the incubation period of recrystallization. Thus, higher dislocation densities in the non-recovered volumes of the samples will lead to higher driving forces for recrystallization. By increasing the numbers of passes up to 8, the mean dislocation density measured immediately after ECAP is increased and accordingly the rate of recrystallization should be faster after larger numbers of passes.

At the same time, the mean dislocation density measured immediately after 16 passes is smaller than after 8 passes and after 4 months the reductions in hardness and flow stress are the highest for the sample processed by 16 passes. This is attributed to the higher degree of recrystallization in this sample. As shown in Section 3.1, processing by ECAP between 8 and 16 passes gives an increase in the twin probability together with a decrease in the total dislocation density. In locations where the twin probability increases at the expense of dislocations, the stored energy will decrease as the twin fault energy in Ag is very low ($\sim 8\,mJ\,m^{-2}$ [15]). Recrystallization may be promoted after 16 passes by the formation of small volumes where the stored energy is much lower than in the neighboring region due to the reduced dislocation/twin den-

sity ratio. These volumes will then act as the embryos for the new grains formed by recrystallization and therefore the time required for grain nucleation will be the shortest for the sample processed by 16 passes. Since in this case the strongly twinned regions are recrystallized first, it follows that there will be a decrease in the twin density in the recovered but non-recrystallized volumes for the sample processed by 16 passes which is in line with the results of X-ray line profile analysis. This is consistent with the observations that the nuclei of recrystallized grains form primarily at deformation twins in low stacking fault energy metals such as Ag [42].

The formation of regions where twinning occurs at the expense of dislocations will increase the degree of inhomogeneity in the microstructure and introduce fluctuations in the stored energy in the sample processed by 16 passes. This is consistent with other studies suggesting that heterogeneities in the microstructure may promote recrystallization due to the higher strain energy gradients [11,43]. It is noted that the high grain boundary energy may also contribute to the driving force for recrystallization in the samples processed by 4–16 passes as the grain size in these materials is smaller (~200 nm) than in the sample processed by only 1 pass (~5 μm). A recent study of annealing in Cu processed by ECAP showed that recrystallization starts heterogeneously primarily in regions where grain boundaries have high angles of misorientation [44]. Since the angle of misorientation at grain boundaries usually increases with increasing numbers of passes in ECAP [22,45], it is reasonable to anticipate that recrystallization in Ag will be faster after larger numbers of passes. Twins can also be regarded as high angle boundaries, therefore the increase of twin density with increasing number of passes may also contribute to faster recrystallization. It is important to note also that impurities have a strong influence on the occurrence of recrystallization during self-annealing. For example, recrystallization was observed in very high-purity (5N) Al even during processing by ECAP at RT [46] which explains the lack of any reports of self-annealing in very high-purity Al. Although, the evolution of texture in Ag during SPD-processing has been investigated by others [47,48], the change in crystallographic texture during self-annealing is a worthwhile subject for future study.

It is noted that self-annealing was also observed previously in ECAP-processed Cu at RT [11,13]. For a similar impurity concentration (~4N), the self-annealing in Ag starts earlier (~1 month) than in Cu (~8 years [13]). As the minimum grain sizes achieved during ECAP are similar (~200 nm) for both Ag and Cu, the grain boundary energy most probably makes a similar contribution to the driving force for recrystallization in the two materials. At the same time, a larger contribution of the lattice strain energy to the driving force for recrystallization yields a faster self-annealing in Ag. Moreover, the lower SFE in Ag is associated with a lower twin fault energy which facilitates the formation of recrystallized embryos. The nuclei formed during recrystallization are usually separated by twins from the parent grains. Therefore, the lower value of the SFE in Ag leads to an easier nucleation of the recrystallized grains which also contributes to faster self-annealing in Ag.

Finally, an important additional consideration from this research is that the reduced stability of ultrafine-grained microstructures in low SFE metals may affect the viability of these materials for use as structural components. To avoid the problems associated with self-annealing, the present research suggests the need to use an optimum and relatively low total strain when applying SPD-processing to pure, low SFE metals. In this way it should be possible to avoid any significant strength degradation during the subsequent service lifetime. It is also suggested to apply alloying which will stabilize the UFG microstructure in low SFE metals for longer time periods.

5. Summary and conclusions

1. Processing by equal-channel angular pressing provides the capability of producing exceptional grain refinement in bulk polycrystalline solids. Self-annealing refers to the recovery and recrystallization occurring in materials processed by ECAP during long-term storage.
2. Experiments were conducted to investigate the occurrence of self-annealing in samples of pure Ag processed by ECAP. The results show the ultrafine-grained microstructure produced by ECAP at room temperature may be unstable in subsequent storage at the same temperature. The driving force for recovery and recrystallization is the high dislocation density developed during ECAP due to the very low stacking fault energy and the high degree of dislocation dissociation.
3. Self-annealing was observed over a period of up to 4 months in samples processed between 4 and 16 passes. No self-annealing was observed in a sample processed through 1 ECAP pass. With increasing numbers of ECAP passes, there is an increase in the contribution from twinning which gives a more heterogeneous microstructure and appears to facilitate recrystallization.

Acknowledgements

This work was supported in part by the Hungarian Scientific Research Fund, OTKA, Grant Nos. K67692 and K71594 (JG and NQC) and in part by the National Science Foundation of the United States under Grants Nos. DMR-0243331 and DMR-0855009 (TGL). In addition, JG is grateful for the support of a Bolyai János Research Scholarship of the Hungarian Academy of Sciences and NQC thanks the Hungarian–American Enterprise Scholarship Fund for support. JG is grateful to Prof. Geza Tichy and Prof. Hael Mughrabi for fruitful discussions. The authors thank Andrea Jakab for preparation of the TEM samples.

References

[1] R.Z. Valiev, R.K. Islamgaliev, I.V. Alexandrov, Prog. Mater. Sci. 45 (2000) 103–189.
[2] Y.T. Zhu, T.C. Lowe, T.G. Langdon, Scripta Mater. 51 (2004) 825–830.
[3] R.Z. Valiev, Y. Estrin, Z. Horita, T.G. Langdon, M.J. Zehetbauer, Y.T. Zhu, JOM 56 (4) (2006) 33–39.
[4] K.B. Yin, Y.D. Xia, C.Y. Chan, W.Q. Zhang, Q.J. Wang, X.N. Zhao, A.D. Li, Z.G. Liu, M.W. Bayes, K.W. Yee, Scripta Mater. 58 (2008) 65–68.
[5] M. Stangl, M. Lipták, A. Fletcher, J. Acker, J. Thomas, H. Wendrock, S. Oswald, K. Wetzig, Microelectron. Eng. 85 (2008) 534–541.
[6] K. Hansen, K. Pantleon, Scripta Mater. 58 (2008) 96–98.
[7] J.-M. Paik, Y.-J. Park, M.-S. Yoon, J.-H. Lee, Y.-C. Joo, Scripta Mater. 48 (2003) 683–688.
[8] B. Gunther, A. Kumpmann, H.-D. Kunze, Scripta Metall. Mater. 27 (1992) 833–838.
[9] V.Y. Gertsman, R. Birringer, Scripta Metall. Mater. 30 (1994) 577–581.
[10] R.Z. Valiev, T.G. Langdon, Prog. Mater. Sci. 51 (2006) 881–981.
[11] G. Wang, S.D. Wu, L. Zuo, C. Esling, Z.G. Wang, G.Y. Li, Mater. Sci. Eng. A 346 (2003) 83–90.
[12] Y. Estrin, N.V. Isaev, S.V. Lubenets, S.V. Malykhin, A.T. Pugachov, V.V. Pustovalov, E.N. Reshetnyak, V.S. Fomenko, L.S. Fomenko, S.E. Shumilin, M. Janecek, R.J. Hellmig, Acta Mater. 54 (2006) 5581–5590.
[13] O.V. Mishin, A. Godfrey, Metall. Mater. Trans. A 39A (2008) 2923–2930.
[14] J. Schamp, B. Verlinden, J. Van Humbeeck, Scripta Mater. 34 (1996) 1667–1672.
[15] J.P. Hirth, J. Lothe, Theory of Dislocations, Wiley, New York, 1982.
[16] J. Gubicza, N.Q. Chinh, J.L. Lábár, Z. Hegedüs, C. Xu, T.G. Langdon, Scripta Mater. 58 (2008) 775–778.
[17] L. Balogh, T. Ungár, Y. Zhao, Y.T. Zhu, Z. Horita, C. Xu, T.G. Langdon, Acta Mater. 56 (2008) 809–820.
[18] Y.H. Zhao, Z. Horita, T.G. Langdon, Y.T. Zhu, Mater. Sci. Eng. A 474 (2008) 342–347.
[19] J. Gubicza, N.Q. Chinh, J.L. Lábár, Z. Hegedűs, P. Szommer, G. Tichy, T.G. Langdon, J. Mater. Sci. 43 (2008) 5672–5676.
[20] Y. Iwahashi, J. Wang, Z. Horita, M. Nemoto, T.G. Langdon, Scripta Mater. 35 (1996) 143–146.
[21] L. Balogh, G. Ribárik, T. Ungár, J. Appl. Phys. 100 (2006) 023512.
[22] M. Kawasaki, Z. Horita, T.G. Langdon, Mater. Sci. Eng. A 524 (2009) 143–150.
[23] P. Müllner, C. Solenthaler, Mater. Sci. Eng. A 230 (1997) 107–115.
[24] J.A. Venables, Philos. Mag. 6 (1961) 379–396.

[25] J.B. Cohen, J. Weertman, Acta Metall. 11 (1963) 996–998.
[26] S. Mahajan, G.Y. Chin, Acta Metall. 21 (1973) 1353–1363.
[27] Y.T. Zhu, X.Z. Liao, S.G. Srinivasan, E.J. Lavernia, J. Appl. Phys. 98 (2005) 034319.
[28] Z.W. Wang, Y.B. Wang, X.Z. Liao, Y.H. Zhao, E.J. Lavernia, Y.T. Zhu, Z. Horita, T.G. Langdon, Scripta Mater. 60 (2009) 52–55.
[29] F. Dalla Torre, R. Lapovok, J. Sandlin, P.F. Thomson, C.H.J. Davies, E.V. Pereloma, Acta Mater. 52 (2004) 4819–4832.
[30] I. Kovács, L. Zsoldos, Dislocations and Plastic Deformation, Pergamon Press, London, 1973.
[31] J. Friedel, Dislocations and Mechanical Properties of Crystals, John Wiley and Sons, New York, 1957.
[32] P.B. Escaig, J. Phys. 29 (1968) 225–239.
[33] A.N. Stroh, Proc. R. Soc. A 2243 (1954) 404–414.
[34] G. Saada, J. Phys. III 1 (1991) 945–956.
[35] T. Ungár, M. Zehetbauer, Scripta Mater. 35 (1996) 1467–1473.
[36] A.S. Argon, W.C. Moffatt, Acta Metall. 29 (1981) 293–299.
[37] S. Schumacher, R. Birringer, R. Straus, H. Gleiter, Acta Metall. 37 (1989) 2485–2488.
[38] J. Gubicza, N.Q. Chinh, T. Csanádi, T.G. Langdon, T. Ungár, Mater. Sci. Eng. A 462 (2007) 86–90.
[39] N.Q. Lam, S.J. Rothman, H. Mehrer, L.J. Nowicki, Phys. Stat. Sol. B 57 (1973) 225–236.
[40] R.E. Hoffmann, D. Turnbull, J. Appl. Phys. 22 (1951) 634–639.
[41] H.P. Stüwe, A.F. Padilha, F. Siciliano, Mater. Sci. Eng. A 333 (2002) 361–367.
[42] H. Paul, J.H. Driver, C. Maurice, A. Piatkowski, Acta Mater. 55 (2007) 575–588.
[43] M. Kumar, A.J. Schwartz, W.E. King, Acta Mater. 50 (2002) 2599–2612.
[44] O.V. Mishin, J.R. Bowen, Metall. Mater. Trans. A 40 (2009) 1684–1692.
[45] S.D. Terhune, D.L. Swisher, K. Oh-ishi, Z. Horita, T.G. Langdon, T.R. McNelley, Metall. Mater. Trans. A 33 (2002) 2173–2184.
[46] W. Skrotzki, N. Scheerbaum, C.-G. Oertel, H.-G. Brokmeier, S. Suwas, L.S. Tóth, Acta Mater. 55 (2007) 2211–2218.
[47] S. Suwas, L.S. Tóth, J.-J. Fundenberger, W. Skrotzki, Scripta Mater. 49 (2003) 1203–1208.
[48] I.J. Beyerlein, L.S. Tóth, C.N. Tomé, S. Suwas, Philos. Mag. 87 (2007) 885–906.